Available online at www.sciencedirect.com
ScienceDirect
Trans. Nonferrous Met. Soc. China 32(2022) 1336−1350
Transactions of Nonferrous Metals Society of China
www.tnmsc.cn

Chromatographic separation and recovery of Zn(II) and Cu(II) from high-chlorine raffinate of germanium chlorination distillation

Ye-hui-zi WU[1], Kang-gen ZHOU[1,2], Wei CHEN[1,2], Qing-yuan LEI[1], Er-jun ZHANG[1], Yu-yao CHENG[1], Yang JIANG[1], Chang-hong PENG[1,2], Jun JIANG[1], Xue-kai ZHANG[1,3]

1. School of Metallurgy and Environment, Central South University, Changsha 410083, China;
2. Chinese National Engineering Research Center for Control & Treatment of Heavy Metal Pollution, Central South University, Changsha 410083, China;
3. School of Chemistry and Chemical Engineering, Central South University, Changsha 410083, China

Received 4 March 2021; accepted 26 October 2021

Abstract: An anion-exchange-based chromatographic separation approach was developed to selectively recover zinc and copper from the high-chlorine raffinate generated in the process of germanium chlorination distillation using 717 resins based on the coordination difference between Zn^{2+}/Cu^{2+} and Cl^{-}. The theoretical calculation and spectroscopic analyses suggested that the coordination between Zn^{2+} and Cl^{-} is much stronger than that between Cu^{2+} and Cl^{-}, and the Cl^{-} concentration significantly affects Zn(II) and Cu(II) species. The factors involving Cl^{-} concentration, resin dosage, shaking speed, and temperature were investigated to determine the optimal condition, and the maximum separation factor of Zn/Cu reached as high as 479.2. The results of the adsorption isotherms, adsorption kinetics, SEM, FTIR, and XPS analyses indicated that the process followed the monolayer uniform chemisorption. Through the continuous adsorption experiments, Zn(II) and Cu(II) in the high-chlorine raffinate were separately recovered, allowing the reuse of residual waste acid and germanium.

Key words: chromatographic separation; Zn/Cu recovery; high-chlorine raffinate; anion exchange; 717 resin

1 Introduction

The scattered metal germanium is the strategic reserve resource with wide applications in high-tech fields attributing to its electrical and optical properties. Globally, approximately 100 t/a of scattered metal germanium is consumed, but its worldwide reserve is only 8600 t [1]. Most of germanium in the lithosphere occurs in trace and minor amounts in various associated minerals, such as Zn in sphalerite and Cu in sulphide deposits. For example, the content of germanium from the zinc plant purification residue in southern China reached (0.2−0.5) wt.%, much higher than that of 0.00067 wt.% (worldwide average in the Earth's crust) [2]. The increasing germanium consumption combined with resource scarcity drives the recovery of germanium from the metallurgical by-products of zinc [3]. Traditionally, germanium is extracted as $GeCl_4$ from the wastes by acidic leaching, chemical precipitation, followed by chlorination distillation, thus generating vast amount of high-chlorine raffinate containing zinc and copper [4]. This toxic and nonbiodegradable high-chlorine raffinate poses potential threat to the environment and human health. It will be ideal to reuse the high-chlorine raffinate in the form of hydrochloric acid to the chlorination distillation stage, realizing the closed loop and avoiding the generation of wastewater. However, the distillation efficiency and purity of $GeCl_4$ were significantly reduced by the presence of

Corresponding author: Xue-kai ZHANG, Tel: +86-18711175301, E-mail: xuekai0102@126.com, xuekai0102@csu.edu.cn
DOI: 10.1016/S1003-6326(22)65878-3

Zn(II) and Cu(II) [5]. Therefore, the removal of Zn(II) and Cu(II) is the key step for the reuse of the raffinate.

Hydroxides and carbonates are widely applied as the precipitant in the treatment of metal-containing wastewater. However, the acids are neutralized rather than reused, and the process produces a large amount of waste sludge [6]. Zinc and copper are valuable metals for global manufacturing industry, and the reserves of these metallic mineral resources are rapidly diminishing. Therefore, selective recovery of Zn(II) and Cu(II) from the raffinate of germanium chlorination distillation is crucial for environmental protection and resource reclamation. Solvent extraction has the advantages of high extraction efficiency, compatibility, and operational simplicity, and the extraction efficiency highly depends on pH, competing ions, and the nature of volatile extractants [7]. The separation recovery of Zn(II) and Cu(II) has been impossible even using commonly used organophosphorus extractant Cyanex 272, amine extractants N1923, and Aliquat 336, because of their tendency to emulsify [8,9]. Membrane separation with low energy consumption can selectively recover metals and avoid sludge disposal problem; however, its stability is significantly affected by the ionic strength, influent quality, and pH [10]. Moreover, traditional adsorption technique for zinc and copper is usually limited in the adsorption capacity, reusability, and costly modification precursor [11]. Thus, ion-exchange technique has been proposed by several studies for the recovery of Zn(II) and Cu(II) from sulfuric acid leaching system with chelating resin or cation resin; however, effectively separating cationic Zn(II) and Cu(II) is impossible attributing to their similar properties [12−14].

Various literature reported the separation of Zn(II) with Cu(II) and other metals involving Co(II), Ni(II), Cd(II), and Fe(III) [15,16]. However, the selective recovery of Zn(II) and Cu(II) from high chloride system by chromatographic separation with anion-exchange resin has been rarely achieved. Notably, the raffinate generated from germanium chlorination distillation contains a high chloride concentration apart from Zn(II) and Cu(II). In this system, the Zn(II) and Cu(II) species may vary significantly due to the difference in coordination capacity based on the previous study [17]. Zn(II) could easily form anionic chloride complexes ($ZnCl_3^-$ and $ZnCl_4^{2-}$) that can be adsorbed by anion-exchange resin even at a reasonably low chloride concentration, compared to Cu(II) [18]. 717 resin with $—N(CH_3)_3Cl$ functional groups has been extensively used as an anion-exchange adsorbent owing to its efficient adsorption efficiency, good stability, facile recoverability, and reusability, making it possible to selectively separate Zn(II) and Cu(II) with 717 resin at an applicable chloride concentration.

Therefore, this study is devoted to separately recover Zn(II) and Cu(II) from the high-chlorine raffinate of germanium chlorination distillation by a chromatographic separation approach based on the difference in Zn/Cu−Cl coordination. The Zn(II) and Cu(II) species in varying chloride concentrations were confirmed based on the thermodynamic calculation and spectroscopic analyses. The effects of chloride concentration, resin dosage, shaking speed, and temperature were investigated to optimize the operational parameters. Subsequently, the adsorption mechanism was elucidated by adsorption isotherms, adsorption kinetics, SEM−EDS, FTIR, and XPS analyses providing auxiliary evidence.

2 Experimental

2.1 Reagents

The 717 resin with quaternary ammonium groups was purchased from Dacheng Ruiyou Chemical Co., Ltd., Zhejiang, China, and its physicochemical properties are listed in Table 1. The resin was successively pretreated with ethanol solution, saturated NaCl solution, 5% NaOH solution, 5% HCl solution, and deionized water. Then, the resin was dried in a vacuum oven at 308 K for 48 h. All other chemicals such as $ZnCl_2$, $CuCl_2·2H_2O$, $CaCl_2$, NaCl, NaOH, and concentrated HCl purchased from Sinopharm Chemical Reagent Co., Ltd., were of analytical grade. Deionized water was used throughout the experiments.

2.2 Adsorption experiments

The experimental procedure is shown in Fig. 1. Batch adsorption experiments were carried out to explore the effect of chloride concentration, resin dosage, shaking speed, and temperature on the separation of Zn(II) and Cu(II) in chloride solution

Table 1 Physicochemical properties of 717 resin

Property	Description or value
Type	Strong basic anion-exchange resin
Matrix structure	Styrene-divinylbenzene copolymer
Solubility	Insoluble in all common solvent
Particle size fraction (0.32−1.25 mm)/%	≥95
Total exchange capacity/(mmol·g^{-1})	≥3.6
Moisture content/%	48−58
Maximum thermal stability/°C	≤80
pH range	0−14

by 717 resin. $ZnCl_2$ and $CuCl_2·2H_2O$ were dissolved at the concentrations of 8 and 2 g/L, respectively, to mimic the actual raffinate of germanium extraction from zinc plant purification residue. Anhydrous calcium chloride was added as the chlorine source to adjust the chloride concentration. Then, the flask was placed on a multiplex magnetic stirrer at 200 r/min for 90 min to ensure reaching coordination equilibrium. Next, a certain amount of 717 resin was added to the solution being stirred at a set temperature and speed.

After completing the adsorption reaction, the solution and 717 resin mixture were collected and analyzed. Two parameters of the equilibrium adsorption capacity Q_e (mg/g) and adsorption efficiency R (%) were used for the description of the adsorption, and calculated by Eqs. (1) and (2), respectively:

$$Q_e=(c_0-c_e)V/(1000m) \quad (1)$$

$$R=[(c_0-c_e)/c_0]\times 100\% \quad (2)$$

where c_0 and c_e are the initial and equilibrium concentrations of Zn(II) or Cu(II) (mg/L), respectively, V (mL) is the volume of solution, and m is the mass of dried resin (g). Additionally, the separation efficiency is described by the selective separation factor $\beta_{Zn/Cu}$ defined as follows:

$$\beta_{Zn/Cu}=\gamma_{Zn}/\gamma_{Cu} \quad (3)$$

$$\gamma_{Me}=(c_0-c_e)/c_e \quad (4)$$

where Me represents Zn or Cu, γ_{Me} is the ratio of metal ion concentrations on the resin and in the solution after adsorption equilibrium. Three parallel tests were carried out and the average value was reported.

Continuous adsorption experiments were performed to evaluate the separation performance

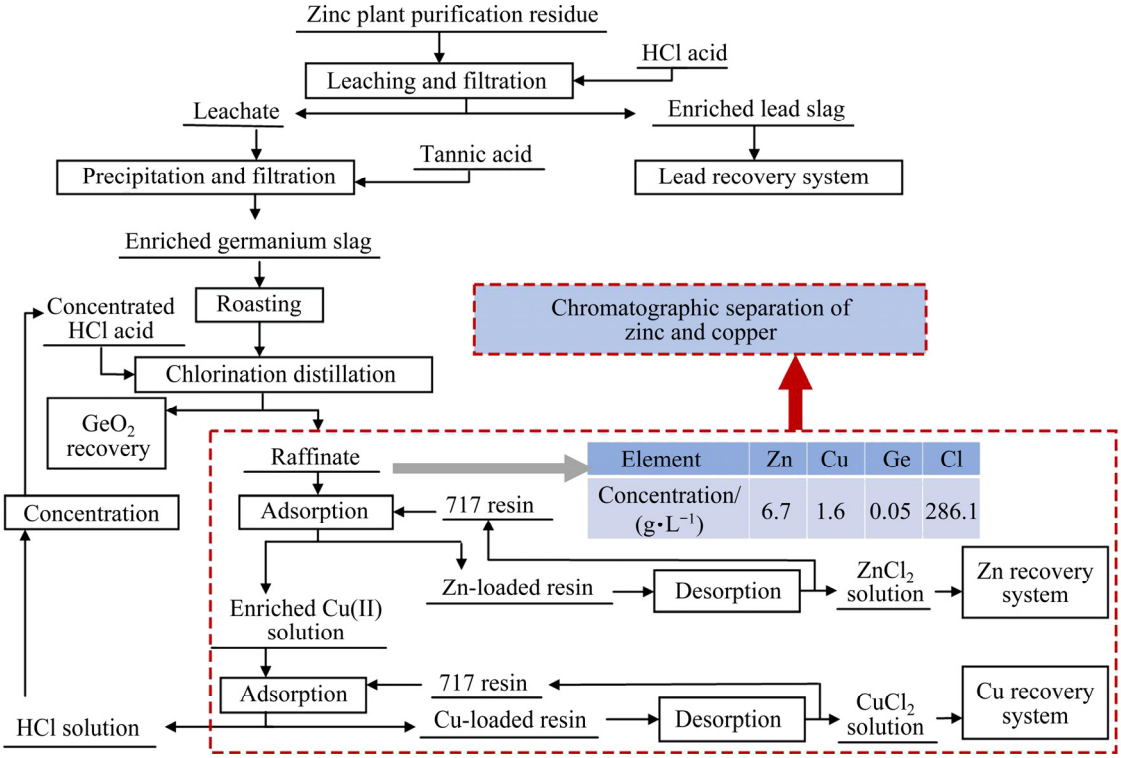

Fig. 1 Experimental procedure for chromatographic separation of valuable components in high-chlorine raffinate of germanium chlorination distillation

of Zn(II) and Cu(II) using a glass column (diameter of 41.2 mm and length of 280.8 mm) wet-filled with quantitative 717 resin. Actual high-chlorine raffinate obtained from Nanjing Zhongzhe Technology Co., Ltd., China, was used as the feed water, and the concentrations of various elements are listed in Table 2. The solution was passed through the column in the upward direction from the bottom to the top at a constant flow of 1 mL/min in the following breakthrough curve experiments. The elution experiments were carried out using deionized water through a metal-loaded bed column in an up-flow mode at room temperature. The effluent was collected at an interval of 10 min, and the concentrations of Zn(II) and Cu(II) were measured.

Table 2 Element concentrations in high-chlorine raffinate of extracting germanium from zinc plant purification residue

Element	Zn	Cu	Ge	Cl	H^+
Concentration/(g·L^{-1})	6.7	1.6	0.05	286.1	7.9*

* mol/L

2.3 Analytical methods

Absorption spectra of the metal chloride complexes were recorded using a UV−Vis spectrophotometer (Shimadzu UV−2600) at 0.5 nm interval. Raman spectra were measured using a Renishaw Invia Raman microscope (Raman-INVIA, UK) at a spectral resolution of 1 cm^{-1}. Fourier transform infrared (FTIR) spectra were recorded using a VERTEX 70 FT-IR (NEXUS-Thermo Nicolet Company, USA). The concentration of metal ions was determined by inductively coupled plasma−atomic emission spectroscopy (ICP−AES, Thermo Scientific ICAP7400 Radial). The microstructure of resin was characterized by scanning electron microscopy (SEM, MIRA3 LMH) and energy-dispersive X-ray spectroscopy (EDS, X MAX20). The chemical composition of the resin surface was investigated by X-ray photoelectron spectroscopy (XPS, Thermo Fisher-VG Scientific ESCALAB250Xi, USA).

3 Results and discussion

3.1 Thermodynamic calculation and reaction mechanism

The forms of species and the corresponding cumulative formation constants of Zn(II) and Cu(II) in chloride system are listed in Table 3 [19,20]. Clearly, Zn(II) readily coordinated with chloride ion to form anionic zinc chloride complexes, while the coordination of Cu(II) was significantly weaker. The reaction and equation can be expressed as follows:

$$Me^{2+}+nCl^-=MeCl_n^{2-n} \quad (5)$$

$$\varphi_n=[MeCl_n^{2-n}]/([Me^{2+}][Cl^-]^n) \quad (6)$$

where $[MeCl_n^{2-n}]$, $[Me^{2+}]$, and $[Cl^-]$ are the concentrations of the corresponding species, respectively, n=1−4; φ_n is the cumulative formation constant.

Table 3 Cumulative formation constants for metal chloride complexes

Metal	Species	lg φ_n			
		n=1	n=2	n=3	n=4
Zn(II)	$ZnCl^+$, $ZnCl_2^0$, $ZnCl_3^-$, $ZnCl_4^{2-}$	0.43	0.61	0.53	0.20
Cu(II)	$CuCl^+$, $CuCl_2^0$, $CuCl_3^-$, $CuCl_4^{2-}$	0.40	−0.69	−2.29	−4.59

The effect of chloride concentration on the forms of metal chloride complexes is illustrated in Figs. 2(a) and (b). The percentage of anionic zinc chloride complexes increases with increasing chloride concentration. Only a few percent exists as Zn^{2+} when the chloride concentration is 2 mol/L, and over 70% of Zn(II) is in the forms of $ZnCl_3^-$ and $ZnCl_4^{2-}$, which can be adsorbed by an anion-exchange resin. However, Cu(II) exists as non-anionic copper species in a wide range of chloride concentration (0.1−7 mol/L). The percentage of Cu(II) species in the form of $CuCl_3^-$ and $CuCl_4^{2-}$ notably increases when the chloride concentration reaches 5 mol/L. Therefore, Zn(II) can be selectively separated in the presence of Cu(II) with anion-exchange resin at an appropriate chloride concentration.

To verify the metal chloride complexes species with the variation of chloride concentration, Raman and UV−Vis spectra of the solution were recorded. Figures 2(c) and (d) show the Raman peaks of Zn/Cu chloride complexes with significant intensity, and are in accordance with our previous thermodynamic calculations that Zn/Cu can coordinate with chloride ion with the increase of

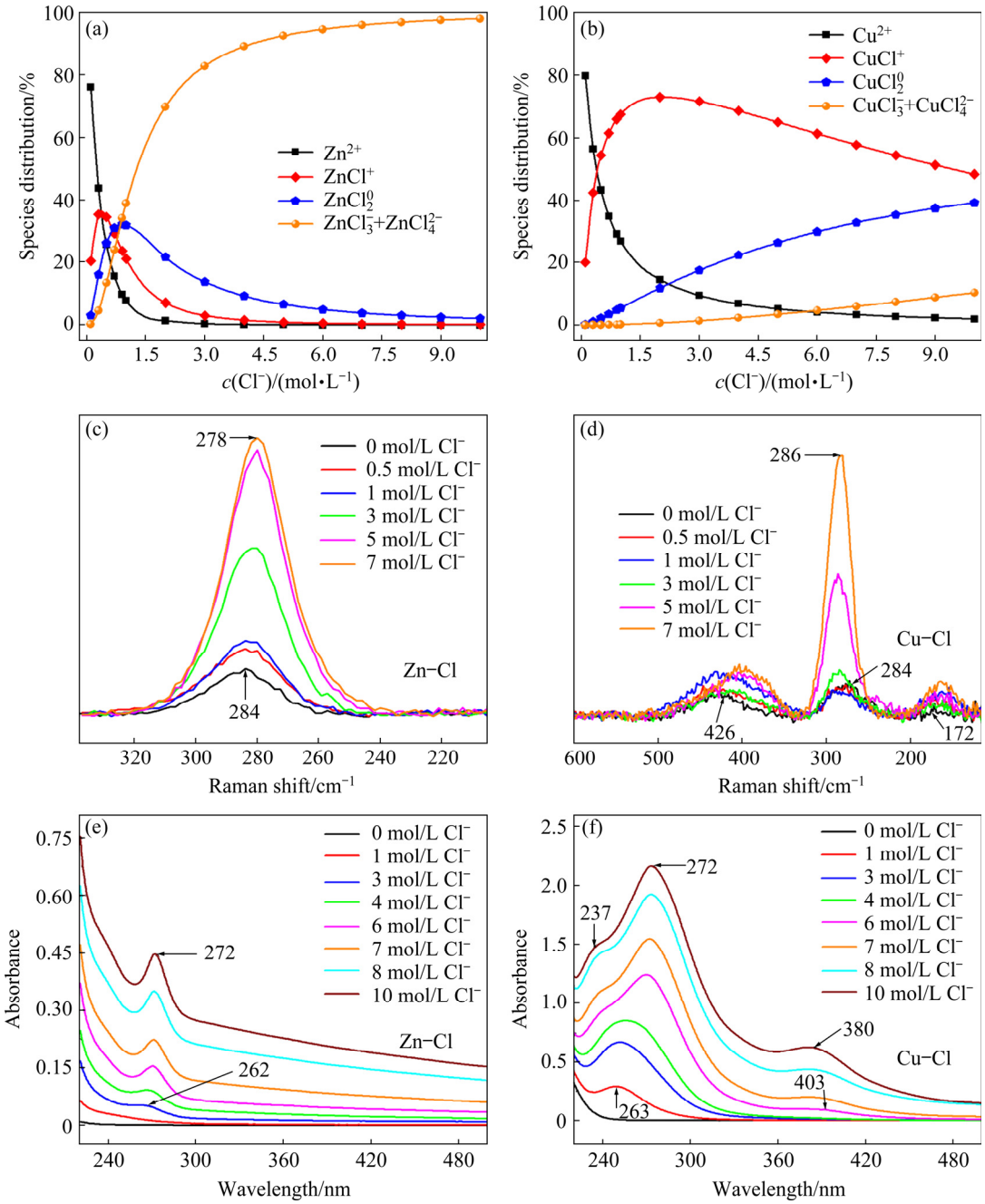

Fig. 2 Distribution of $MeCl_2$ species (a, b), changes of Raman spectra with 1 mol/L $MeCl_2$ (c, d), and UV−Vis spectra with 0.001 mol/L $MeCl_2$ for metal chloride complexes (e, f) under different chloride concentrations at 298 K

chloride concentration. As shown in Fig. 2(c), the concentration of additional chlorine species increased from 0 to 1 mol/L, and a predominant band appeared at 284 cm^{-1}, corresponding to $ZnCl_2^0$ [21]. Further increasing the chlorine concentration resulted in a band red-shift to 278 cm^{-1}, which can be assigned to the peak of $ZnCl_4^{2-}$ [22]. For Cu, when the chloride concentration increased from 3 to 5 mol/L, the band at 284 cm^{-1} shifted to 286 cm^{-1} and its intensity sharply increased, and can be ascribed to the increase of $CuCl_4^{2-}$ complexes considering the thermodynamic calculation shown in Fig. 2(b). The other two bands of Cu−Cl at 426 and 172 cm^{-1} showed negligible change in peak intensity with increasing chlorine content, and can be assigned to $CuCl_2^0$ (Fig. 2(d)) [23].

UV−Vis spectroscopy was also used to identify the speciation of metal chloride complexes in aqueous solution. Continuous increase in absorbance was observed with increasing chlorine concentration from 0 to 10 mol/L (Figs. 2(e) and

(f)). For Zn(II)−Cl system, the peak at 262 nm appeared and red-shifted to 272 nm, when the chloride concentration constantly increased to 10 mol/L (Fig. 2(e)). The peak at 272 nm was assigned to $ZnCl_4^{2-}$ species as it is the steadiest state in chloride solution [24]. As for Cu(II)−Cl system, the absorbance also increased with increasing chloride concentration, while the peaks appeared at different wavelengths. With increasing chloride concentration, a peak at 403 nm appeared (chloride concentration of 6 mol/L) and gradually blue-shifted to 380 nm (chloride concentration of 10 mol/L), which can be attributed to the tetrahedral $CuCl_4^{2-}$ complexes (Fig. 2(f) [25]. The absorption peak at 263 nm indicated the fully hydrated Cu^{2+} ions, and split into two new peaks at 237 and 272 nm with increasing chloride concentration, suggesting the coordination of Cu(II) with chloride ion [26]. Zn(II) has a larger radius of the central ions (74 Å) than Cu(II) (72 Å), and may result in a stronger coordination capacity of Zn(II) to chloride ion. Therefore, the coordination of Zn(II) and Cu(II) with chloride ion is significantly discrepant, and the key of separating the two metals is to control the chloride concentration.

These results show that it is feasible to keep Zn(II) species in the form of $ZnCl_3^-$ and $ZnCl_4^{2-}$ anions, while Cu(II) species as cations by adjusting the chloride concentration, and the subsequent separation would be easy by the anion-exchange method. 717 resin has high adsorption capacity, low cost, stable physicochemical properties, and industrial universalities, and thus was selected as the adsorbent for the chromatographic separation of Zn(II) and Cu(II) in chloride solution. The adsorption reaction, depending on the chloride concentration in the system, can be represented as follows:

$$(n-2)[RN(CH_3)_3Cl]+MeCl_n^{2-n} \rightarrow [RN(CH_3)_3]_{n-2}MeCl_n+(n-2)Cl^- \quad (7)$$

3.2 Adsorption equilibrium

The previous results demonstrated that the chloride concentration can significantly affect the distribution of Zn(II) and Cu(II) species, and thus affects the adsorption performance of Zn(II) and Cu(II). Equilibrium experiments were conducted to investigate the effects of chloride concentration, resin dosage, shaking speed, and temperature on the adsorption and separation of Zn(II) and Cu(II), and the results are shown in Fig. 3. The adsorption efficiency of Zn(II) increased from 69% to 97% with constantly increasing chloride concentration from 0.3 to 2.8 mol/L, and reached equilibrium afterwards. The maximum adsorption capacity of Zn(II) reached 51.9 mg/g (Fig. 3(a)). In comparison, the adsorption efficiency of Cu(II) was much lower despite a gradual increase with increasing chloride concentration because the formation of anionic zinc chloride complexes was stronger than that of copper chloride complexes at the same chloride concentration, which is consistent with the results in Fig. 2. Furthermore, the selective separation factor ($\beta_{Zn/Cu}$) sharply increased with increasing chloride concentration from 0.3 to 2.8 mol/L, and pronouncedly decreased afterwards. The value of $\beta_{Zn/Cu}$ reached up to 479.2 when the chloride concentration was 2.8 mol/L. As a result, 717 resin can be used to selectively separate Zn(II) and Cu(II) from aqueous chloride solution at an appropriate chloride concentration. Therefore, the chloride concentration was set to be 2.8 mol/L for the subsequent experiments.

The effect of resin dosage on the adsorption and separation of Zn(II) and Cu(II) is shown in Fig. 3(b). The Zn(II) adsorption efficiency increased from 13% to 97% with increasing resin dosage from 1 to 11 g, attributed to the increasing amount of active sites and exchangeable ions available for adsorption. In comparison, the adsorption capacity of Zn(II), which was 107.4 mg/g at the resin dosage of 1 g, decreased with increasing resin dosage from 3 to 14 g. The reason might be the partial overlapping or aggregation of 717 resin, decreasing the total surface area and the availability of sorption sites. As for Cu(II), less than 7% of Cu(II) was adsorbed with the resin dosage of 11 g, and the $\beta_{Zn/Cu}$ was 479.2. As a result, the optimal value of 717 resin dosage was 11 g.

The effects of shaking speed and temperature on the adsorption efficiency of Zn(II) and Cu(II) were also evaluated, and the results are shown in Figs. 3(c) and (d), respectively. The shaking speed had no significant effect on the selective separation. Therefore, the optimal shaking speed was set to be 180 r/min, keeping the energy consumption and operational simplicity in mind. The adsorption efficiency of Zn(II) slowly decreased with the

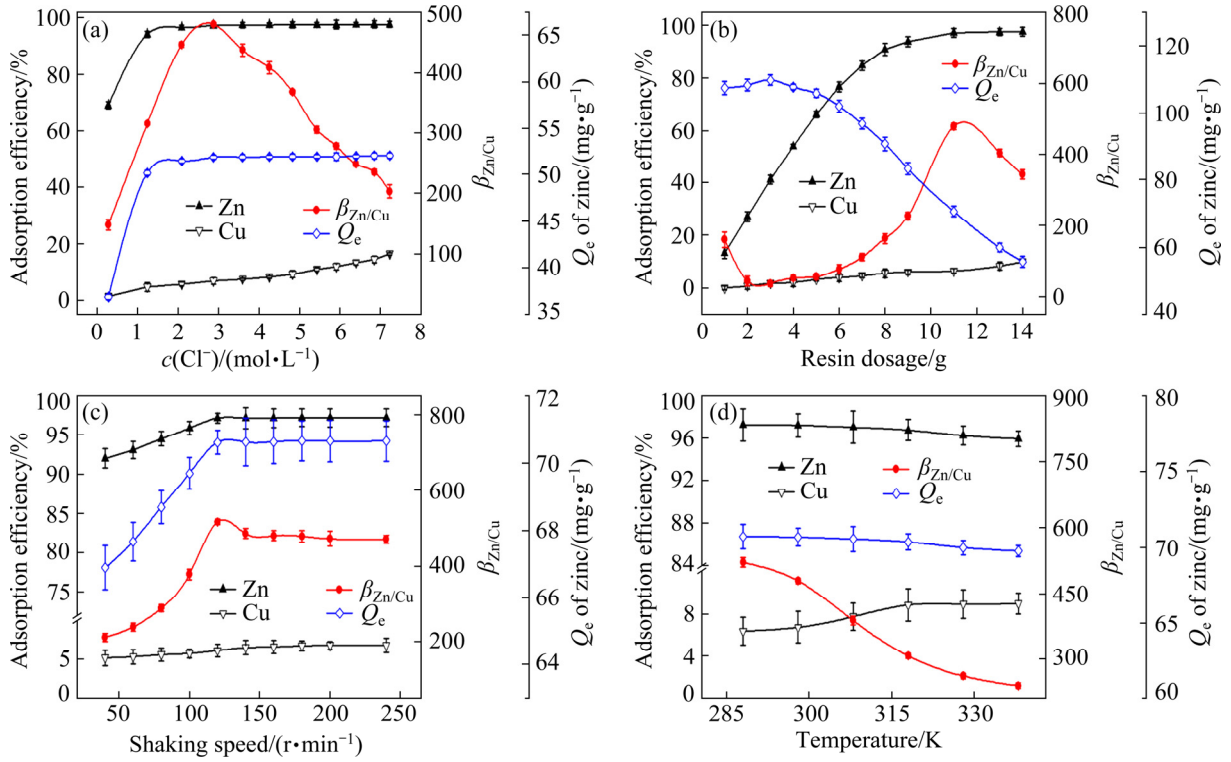

Fig. 3 Effects of different conditions on separation of Zn(II) and Cu(II) with 100 mL simulated solution: (a) Chloride concentration (Resin dosage: 15 g; shaking speed: 180 r/min; temperature: 298 K); (b) Resin dosage (Chloride concentration: 2.8 mol/L; shaking speed: 180 r/min; temperature: 298 K); (c) Shaking speed (Chloride concentration: 2.8 mol/L; resin dosage: 11 g; temperature: 298 K); (d) Temperature (Chloride concentration: 2.8 mol/L; resin dosage: 11 g; shaking speed: 180 r/min)

increase of temperature, while the adsorption efficiency of Cu(II) showed an opposite trend. It can be ascribed to the desorption of zinc chloride complexes caused by an increase in the available thermal energy, because higher temperature induces higher mobility of the adsorbate, which causes desorption. The increasing Cu(II) adsorption efficiency can be explained by the strong coordination of copper chloride complexes. The value of $\beta_{Zn/Cu}$ was 479.2 at 298 K. Therefore, the adsorption temperature was fixed at room temperature (298 K).

3.3 Adsorption isotherms

To further understand the rationale of the adsorption process, adsorption isotherms were used to describe the adsorption behavior [27]. The results shown in Fig. 4(a) indicate the absence of driving force and the unsaturated adsorbing sites at low concentrations. Furthermore, Langmuir and Freundlich models were used to evaluate the adsorption performance of Zn(II) and Cu(II) on 717 resin and expressed as follows:

$$c_e/Q_e=1/(K_LQ_m)+c_e/Q_m \quad (8)$$

$$\ln Q_e=\ln K_f+(1/n)\ln c_e \quad (9)$$

$$R_L=1/(1+K_Lc_i) \quad (10)$$

where c_i (mg/L) and Q_m (mg/g) are the initial maximum concentration of metal ions and the maximum adsorption capacity, respectively; K_L (L/mg) and K_f (mg/g) are the Langmuir and Freundlich constants related to adsorption energy, respectively; n is a parameter to evaluate the favorableness of the adsorption process; R_L is a dimensionless separation coefficient to characterize the stability of the whole adsorption system. If $R_L>1$, the isotherm is unfavorable; if $0<R_L<1$, the isotherm is favorable; if $R_L=0$, the isotherm is irreversible; if $R_L=1$, the isotherm is linear.

The results in Fig. 5 and Table 4 suggest that Langmuir model fitted well for both Zn(II) and Cu(II) adsorption with the correlation coefficients higher than 0.997. Therefore, both Zn(II) and Cu(II)

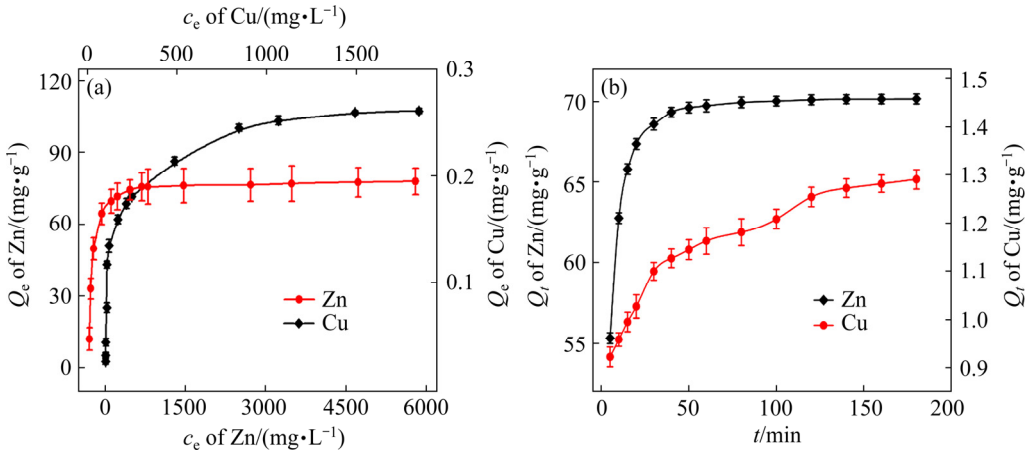

Fig. 4 Adsorption isotherms of Zn(II) and Cu(II) on 717 resin (Zinc concentration: 20−7000 mg/L; copper concentration: 10−2000 mg/L; chloride concentration: 2.8 mol/L; resin dosage: 1 g; shaking speed: 180 r/min; temperature: 298 K) (a) and adsorption kinetic curves of Zn(II) and Cu(II) on 717 resin (Zinc concentration: 8000 mg/L; copper concentration: 2000 mg/L; chloride concentration: 2.8 mol/L; resin dosage: 11 g; shaking speed: 180 r/min; temperature: 298 K) (b)

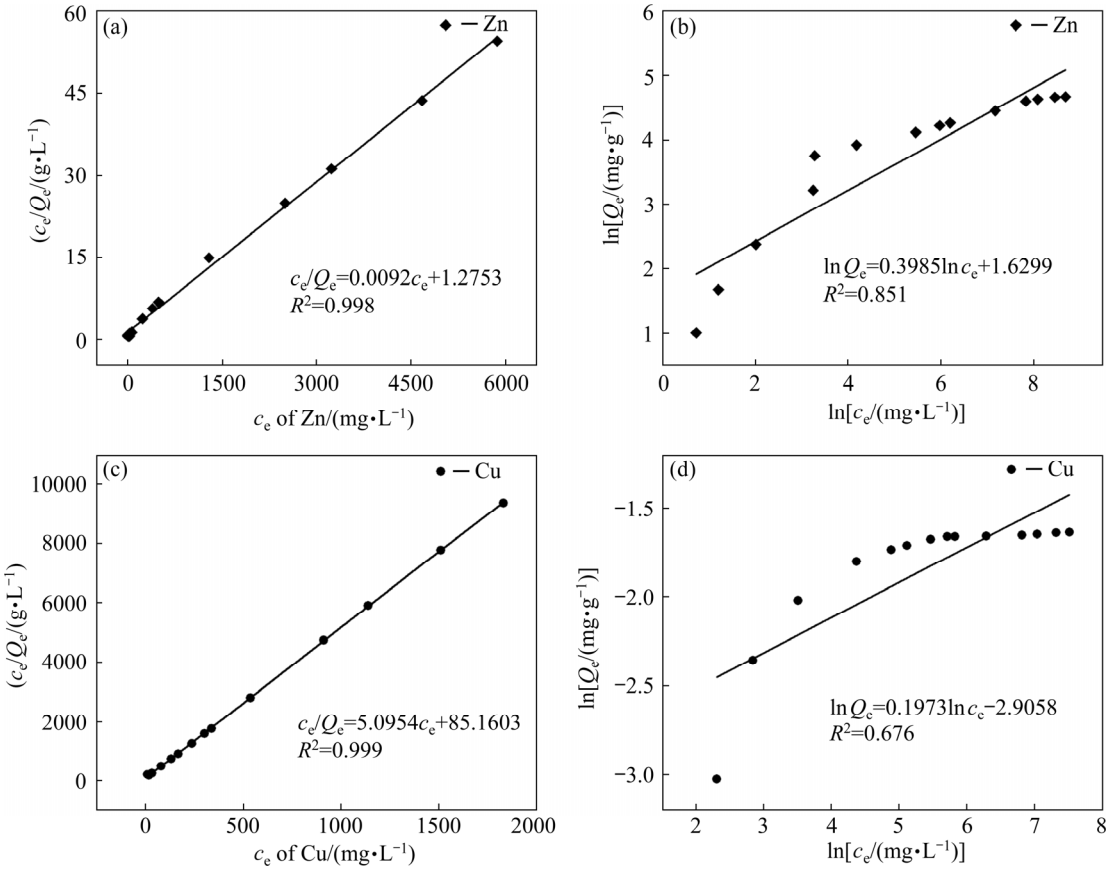

Fig. 5 Adsorption isotherms fitting of corresponding metals on 717 resin: (a, c) Langmuir model; (b, d) Freundlich model

were adsorbed in the form of monolayer, as Langmuir isotherm is a commonly applied model for adsorption on a completely homogenous surface with negligible interaction between adsorbed molecules [28]. Furthermore, the values of R_L were in the range 0−1, indicating that the adsorption process was favorable. In addition, the theoretical maximum adsorption capacity of Zn(II) and Cu(II) calculated by Eq. (8) was 108.7 and 0.2 mg/g, respectively, demonstrating the feasibility

Table 4 Parameters of adsorption isotherms and adsorption kinetics of Zn(II) and Cu(II)

Model	Parameter	Zn(II)	Cu(II)
Langmuir	K_L/(L·mg^{-1})	0.007	0.060
	Q_m/(mg·g^{-1})	108.7	0.2
	R_L	0.020	0.009
	R^2	0.998	0.999
Freundlich	K_f/(mg·g^{-1})	5.103	0.055
	1/n	0.399	0.197
	R^2	0.851	0.676
Pseudo-first-order model	K_1/ min^{-1}	0.011	0.002
	Q_e/(mg·g^{-1})	5.6	1.4
	R^2	0.615	0.877
Pseudo-second-order model	K_2/(g·mg^{-1}·min^{-1})	0.014	0.137
	Q_e/(mg·g^{-1})	70.9	1.3
	R^2	0.999	0.999

of separating Zn(II) and Cu(II) in the chloride solution with 717 resin.

3.4 Adsorption kinetics

Adsorption kinetics was used to describe the adsorption process, interpret the transportation of adsorbate in adsorbents, and further elucidate the dominant adsorption mechanism [29]. As shown in Fig. 4(b), the amount of Zn(II) adsorbed onto the 717 resin sharply increased in 20 min, followed by a decrease in the adsorption rate and finally reached saturation after 120 min. At the adsorption equilibrium, the adsorption capacity of Zn(II) and Cu(II) was 70.2 and 1.3 mg/g, respectively. The fluctuation of the adsorption rate resulted from decreasing number of available binding sites with increasing time. The optimal contact time was 120 min, in the view of the energy consumption and operational simplicity. The adsorption kinetic data were fitted with the pseudo-first-order model and pseudo-second-order model, expressed by Eqs. (11) and (12), respectively:

$$\ln (Q_e-Q_t)=\ln Q_e-K_1t \quad (11)$$

$$t/Q_t=1/(K_2Q_e^2)+t/Q_e \quad (12)$$

where K_1(min^{-1}) and K_2 (g·mg^{-1}·min^{-1}) are the rate constants of the pseudo-first-order model and pseudo-second-order model, respectively.

The fitting results of Zn(II) and Cu(II) are shown in Fig. 6 and Table 4, suggesting that the pseudo-second-order model was better with the higher correlation coefficient (R^2=0.999). Chemisorption was determined as the rate- determining step, suggesting that the adsorption behavior might involve the valency forces sharing electrons of metal ions and 717 resin. Moreover, the Q_e values of Zn(II) and Cu(II) calculated by Eq. (12) were 70.9 and 1.3 mg/g, respectively, which were in agreement with the experimental data.

3.5 Continuous adsorption results

To further test the separation performance and the practical applicability, continuous adsorption experiments were conducted using the actual high-chlorine raffinate of germanium extraction with Zn(II) and Cu(II) of 6.7 and 1.6 g/L, respectively. A variation in the color of resin bed from white to greenish yellow and from the bottom to the top was observed during the adsorption process, and finally changed to white again (Fig. 7(a)). This can be explained by the following process: at the initial stage, the active sites were available for both Zn(II) and Cu(II), but the adsorbed Cu(II) would be replaced by zinc chloride complexes with continuous injection. As a result, the copper species continuously were enriched in the effluent after 0.85 L, and the concentration even reached twice of the initial concentration in the influent. When the adsorption of Zn(II) by 717 resin reached saturation, the Cu(II) concentration in the effluent subsequently decreased until the initial concentration (Fig. 7(b)). The fluid volume was 1.75 L before the Zn(II) breakthrough point, and after that the concentration of Zn(II) dramatically increased. Moreover, the elution curves of metal-loaded resin with the fluid volumes of 2.75 and 0.85 L are presented in Figs. 7(c) and (d), respectively. Clearly, Zn(II) and Cu(II) are effectively separated and enriched during the desorption process.

To further elucidate the feasibility of recovery of Cu(II) with 717 resin, continuous adsorption experiments were performed using the high-chlorine raffinate after zinc removal, and the results are shown in Fig. 8. Apparently, 717 resin effectively adsorbed Cu(II) in the absence of Zn(II), and the resin achieved saturation after 1.50 L. The maximum Cu(II) concentration in the effluent was

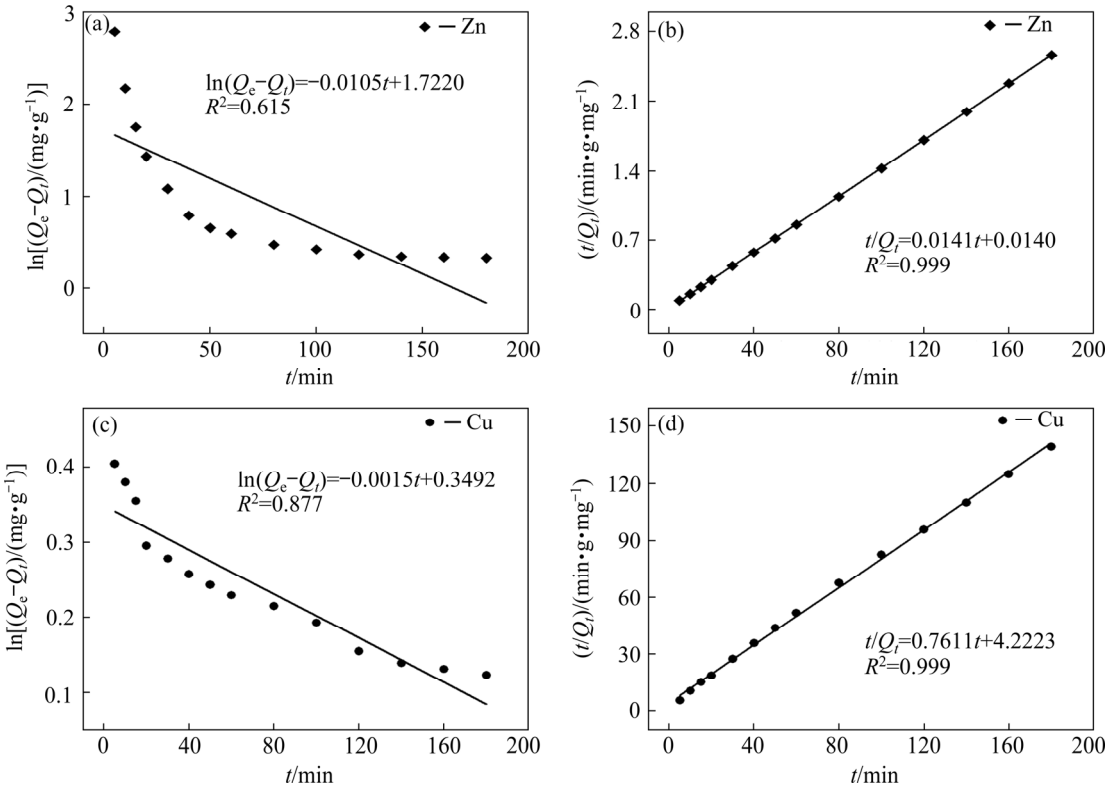

Fig. 6 Adsorption kinetics fitting of corresponding metals on 717 resin: (a, c) Pseudo-first-order model; (b, d) Pseudo-second-order model

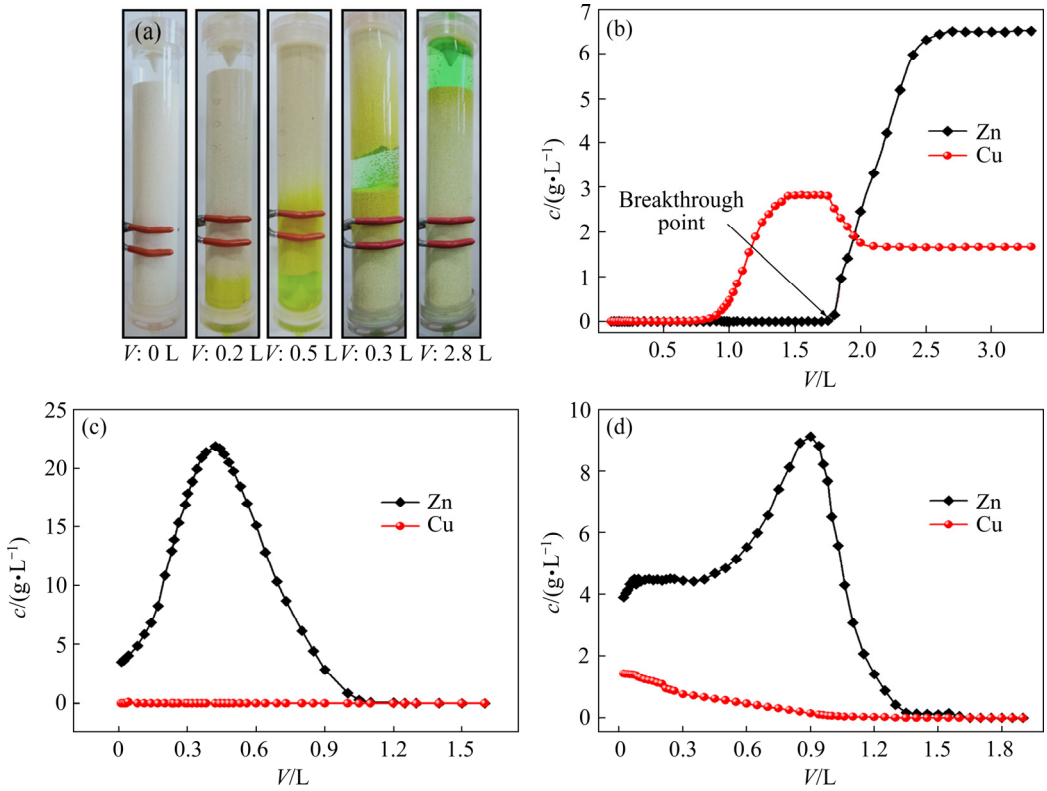

Fig. 7 Color change of resin bed during adsorption process (a), breakthrough curves of 717 resin for wastewater of germanium extraction from zinc refinery residue (b), elution curves of metal-loaded resin with fluid volume of 2.75 L (c), and elution curves of metal-loaded resin with fluid volume of 0.85 L (d)

enriched by 2.90 times compared with that of the feed solution. After the elution process, the resin bed was regenerated and showed excellent reusability in consecutive adsorption/desorption cycles.

3.6 SEM images

The surface morphologies and elemental mass fractions of 717 resin and metal-loaded resin with the fluid volume of 2.75 L were obtained by SEM−EDS (Fig. 9). The structure of 717 resin scarcely changed after adsorbing the metal chloride complexes in the high-chlorine raffinate, while a rougher surface was clearly observed (Figs. 9(d)

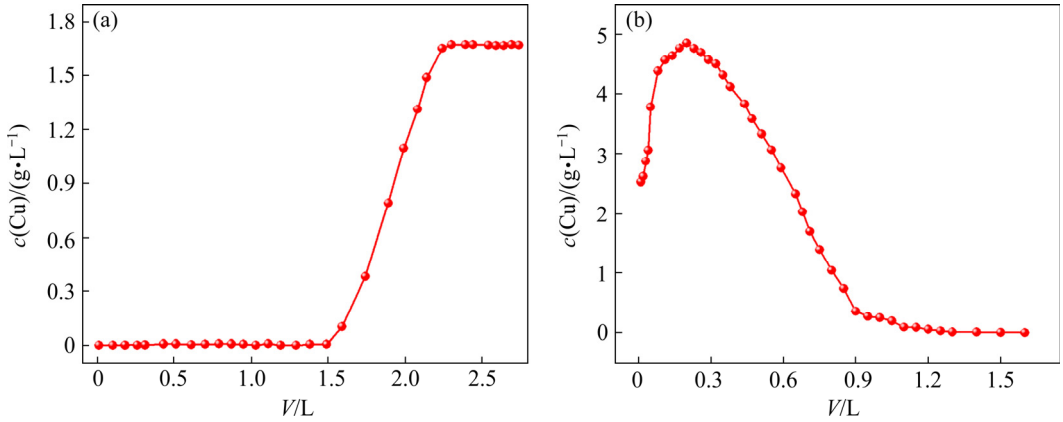

Fig. 8 Breakthrough curve of 717 resin for high-chlorine raffinate of germanium chlorination distillation process after zinc removal (a), and elution curve of Cu-loaded resin (b)

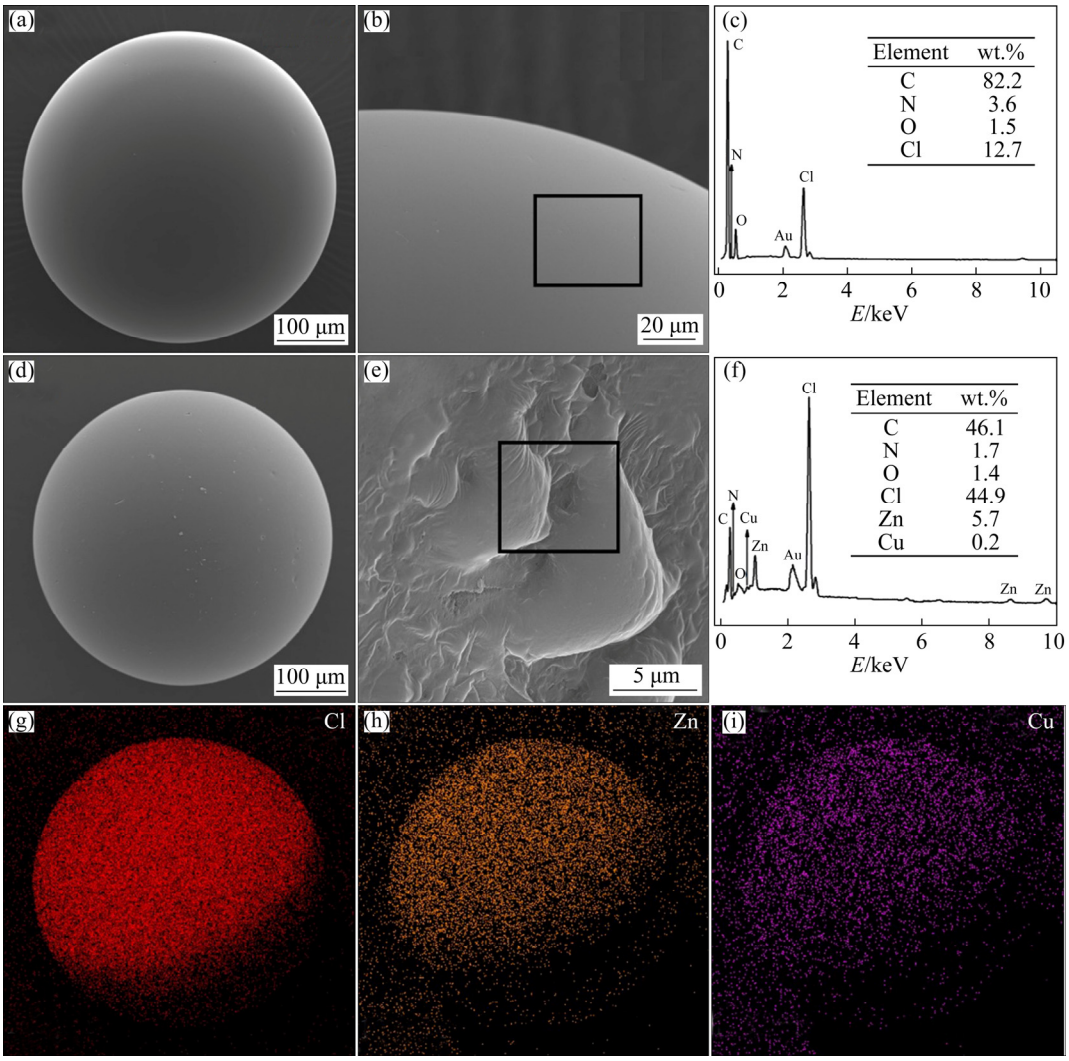

Fig. 9 SEM images and EDS results of 717 resin (a−c), metal-loaded resin with fluid volume of 2.75 L (d−f), and elemental mapping of metal-loaded 717 resin (g−i)

and (e)). Figure 9(f) shows the mass fractions of Zn and Cu, further indicating that Zn(II) could be selectively separated in the presence of Cu(II). Zn(II) and Cu(II) were uniformly adsorbed and dispersed on the 717 resin, as demonstrated by the elemental mapping (Figs. 9(g−i)).

3.7 FTIR spectra

The FTIR spectra of 717 resin before and after metal loading were analyzed to identify the change of functional groups, as shown in Fig. 10. The spectra showed mild peaks at 3456 and 3442 cm^{-1}, respectively, attributing to the stretching vibration of the hydroxyl groups. The stretching vibration peak at 1635 cm^{-1} corresponded to the benzene skeleton [30]. The absorption peak of —$N(CH_3)_3Cl$ at 978 cm^{-1} of the 717 resin slightly shifted to 975 cm^{-1} after the adsorption, resulting from the replacement of chlorine with metal chloride complexes.

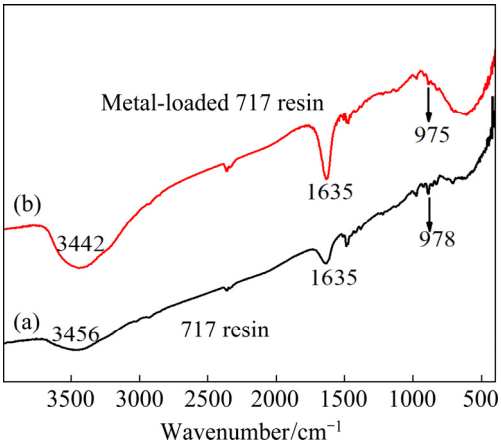

Fig. 10 FTIR spectra of 717 resin (a), and metal-loaded 717 resin with fluid volume of 2.75 L (b)

3.8 XPS spectra

The chemical compositions of the 717 resin were characterized by XPS to further investigate the reaction mechanism between the resin and metal chloride complexes, and the results are shown in Fig. 11. The resin showed the characteristic Zn and Cu peaks after metal loading, while the oxygen content may originate from the ethanol and water molecules remained on the surface even after the sample drying (Fig. 11(a)).

The peaks of C, Cl, N, Zn, and Cu were further fitted to analyze the chemical states of each element. As shown in Fig. 11(b), the peaks at 284.81, 285.60, and 286.42 eV were ascribed to the C—C, C—O, and C—N, respectively [31]. The Cl 2p region of the spectrum (Fig. 11(c)) can be described with the Cl $2p_{1/2}$/Cl $2p_{3/2}$ doublets at 198.71/197.10 eV, which shifted to 200.02/198.43 eV and 199.87/198.22 eV after adsorption of Zn(II) and Cu(II), respectively, demonstrating the coordination of chloride with elements with higher binding energies [32]. Moreover, the intensity of Cl 2p significantly increased due to the introduction of the metal chloride complexes. The N 1s spectrum (Fig. 11(d)) of the 717 resin was divided into two peaks at 399.39 and 402.41 eV, corresponding to the binding energies of N—C and N—Cl, respectively [33]. The N—Cl peak diminished after adsorption, and the peaks of N—Zn at 402.86 eV and N—Cu at 402.65 eV appeared. These results demonstrated that the 717 resin formed bonds with Zn and Cu metals, indicating the strong chemisorption of 717 resin to the metal chloride complexes.

After metal loading, the resin showed pronounced Zn peaks at 1045.63 and 1022.63 eV (Zn $2p_{1/2}$ and Zn $2p_{3/2}$, respectively), while the Cu 2p peaks were negligible, suggesting that Cu was not adsorbed on the resin in the presence of Zn [34]. Nevertheless, when the high-chlorine raffinate after zinc removal was adsorbed by the 717 resin, the characteristic peaks of Cu $2p_{1/2}$ and Cu $2p_{3/2}$ at 952.82 and 933.16 eV appeared, suggesting that Cu(II) can also be adsorbed by 717 resin in the absence of Zn(II) [23]. Therefore, the nitrogen in the —$N(CH_3)_3Cl$ coordinated with the metal chloride complexes, and Zn(II) had a much stronger coordination affinity than Cu(II) towards resin loading.

4 Conclusions

(1) The newly developed anion-exchange-based chromatographic separation approach selectively recovered zinc, copper, and waste acid from high-chlorine raffinate of germanium chlorination distillation. The closed loop of water and the enrichment of germanium were realized, thus increasing the economic benefits.

(2) The distribution of Zn(II) and Cu(II) species under varying chloride concentrations was justified based on the thermodynamic calculation and spectroscopic analyses. Anionic zinc chloride complexes existed as the dominant species at the

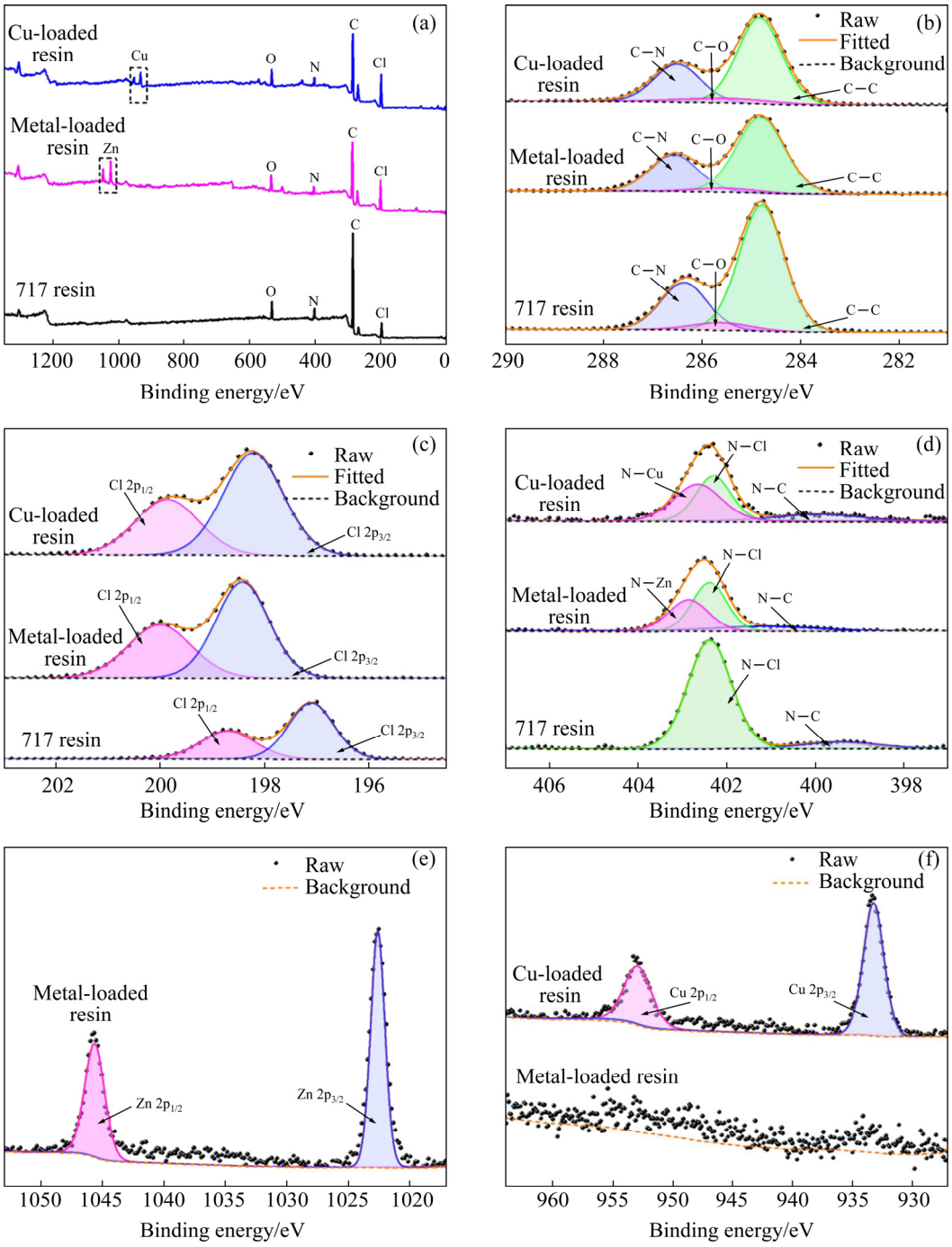

Fig. 11 XPS spectra of 717 resin, metal-loaded resin with fluid volume of 2.75 L, and Cu-loaded resin (a), and high-resolution spectra (b−f) in C 1s (b), Cl 2p (c), N 1s (d), Zn 2p (e) and Cu 2p (f)

chloride concentration higher than 2 mol/L.

(3) The optimal parameters for the selective separation of Zn(II) and Cu(II) are as follows: chloride concentration of 2.8 mol/L, resin dosage of 11 g, shaking speed of 180 r/min, and temperature of 298 K. Under this optimized condition, the adsorption efficiencies of Zn(II) and Cu(II) were 97% and 6%, respectively.

(4) The adsorption isotherms showed that both Zn(II) and Cu(II) followed the monolayer Langmuir model. Moreover, the adsorption kinetics indicated that the process was controlled by chemisorption. Furthermore, the SEM−EDS, FTIR, and XPS analyses revealed that the chemisorption was controlled by the coordination of nitrogen in 717 resin and metal chloride complexes.

(5) This study provides a waste-free and economic method for the selective recovery of Zn(II) and Cu(II) from high-chloride content solution, and may have a prospect of industrial utilization attributing to its full reuse for valuable components.

Acknowledgments

This work was financially supported by the Postdoctoral Research Foundation of Central South University, China (No. 140050037).

References

[1] ZHANG Lin-gen, XU Zhen-ming. Application of vacuum reduction and chlorinated distillation to enrich and prepare pure germanium from coal fly ash [J]. Journal of Hazardous Materials, 2017, 321: 18−27.

[2] RAO Shuai, WANG Dong-xing, LIU Zhi-qiang, ZHANG Kui-fang, CAO Hong-yang, TAO Jin-zhang. Selective extraction of zinc, gallium, and germanium from zinc refinery residue using two stage acid and alkaline leaching [J]. Hydrometallurgy, 2019, 183: 38−44.

[3] RAO Shuai, LIU Zhi-qiang, WANG Dong-xing, CAO Hong-yang, ZHU Wei, ZHANG Kui-fang, TAO Jin-zhang. Hydrometallurgical process for recovery of Zn, Pb, Ga, and Ge from Zn refinery residues [J]. Transactions of Nonferrous Metals Society of China, 2021, 31: 555−564.

[4] SOEEZI A, ABDOLLAHI H, SHAFAEI S Z, RAHIMI E. Extraction and stripping of Cu and Ni from synthetic and industrial solutions of Sarcheshmeh Copper Mine containing Cu, Ni, Fe, and Zn ions [J]. Transactions of Nonferrous Metals Society of China, 2020, 30: 518−534.

[5] NGUYEN T H, LEE M S. A review on germanium resources and its extraction by hydrometallurgical method [J]. Mineral Processing and Extractive Metallurgy Review, 2021, 42: 406−426.

[6] HU Bin, YANG Tian-zu, LIU Wei-feng, ZHANG Du-chao, CHEN Lin. Removal of arsenic from acid wastewater via sulfide precipitation and its hydrothermal mineralization stabilization [J]. Transactions of Nonferrous Metals Society of China, 2019, 29: 2411−2421.

[7] CORREA M M J, SILVAS F P C, ALIPRANDINI P, de MORAES V T, DREISINGER D, ESPINOSA D C R. Separation of copper from a leaching solution of printed circuit boards by using solvent extraction with D2EHPA [J]. Brazilian Journal of Chemical Engineering, 2018, 35: 919−930.

[8] VÁZQUEZ M I, ROMERO V, FONTÀS C, ANTICÓ E, BENAVENTE J. Polymer inclusion membranes (PIMs) with the ionic liquid (IL) Aliquat 336 as extractant: Effect of base polymer and IL concentration on their physical-chemical and elastic characteristics [J]. Journal of Membrane Science, 2014, 455: 312−319.

[9] MISHRA R K, ROUT P C, SARANGI K, NATHSARMA K C. Solvent extraction of zinc, manganese, cobalt, and nickel from nickel laterite bacterial leach liquor using sodium salts of TOPS-99 and Cyanex 272 [J]. Transactions of Nonferrous Metals Society of China, 2016, 26: 301−309.

[10] SONG Jian-feng, HUANG Tao, QIU Hong-bin, NIU Xu-hong, LI Xue-mei, XIE Ying-ming, HE Tao. A critical review on membrane extraction with improved stability: Potential application for recycling metals from city mine [J]. Desalination, 2018, 440: 18−38.

[11] WANG Zhen, LI Tian-xiao, LIU Dong, FU Qiang, HOU Ren-jie, LI Qing-lin, CUI Song, LI Mo. Research on the adsorption mechanism of Cu and Zn by biochar under freeze-thaw conditions [J]. Science of the Total Environment, 2021, 774: 145194.

[12] BOTELHO JUNIOR A B, JIMÉNEZ CORREA M M, ESPINOSA D C R, DREISINGER D, TENÓRIO J A S. Recovery of Cu(II) from nickel laterite leach using prereduction and chelating resin extraction: Batch and continuous experiments [J]. The Canadian Journal of Chemical Engineering, 2019, 97: 924−929.

[13] VECINO X, REIG M, LÓPEZ J, VALDERRAMA C, CORTINA J L. Valorisation options for Zn and Cu recovery from metal influenced acid mine waters through selective precipitation and ion-exchange processes: Promotion of on-site/off-site management options [J]. Journal of Environmental Management, 2021, 283: 112004.

[14] BOTELHO JUNIOR A B, DREISINGER D B, ESPINOSA D C R. A review of nickel, copper, and cobalt recovery by chelating ion exchange resins from mining processes and mining tailings [J]. Mining, Metallurgy & Exploration, 2019, 36: 199−213.

[15] PYSZKA I, RADZYMINSKA-LENARCIK E. New polymer inclusion membrane in the separation of nonferrous metal ion from aqueous solutions [J]. Membranes, 2020, 10: 385.

[16] BARI M F, HOSSAIN M S, MUJTABA I M, JAMALUDDIN S B, HUSSIN K. Simultaneous extraction and separation of Cu(II), Zn(II), Fe(III) and Ni(II) by polystyrene micro- capsules coated with Cyanex 272 [J]. Hydrometallurgy, 2009, 95: 308−315.

[17] BOGACKI M B, ZHIVKOVA S, KYUCHOUKOV G, SZYMANOWSKI J. Modeling of copper(II) and zinc(II) extraction from chloride media with KELEX 100 [J]. Industrial & Engineering Chemistry Research, 2000, 39: 740−745.

[18] ZHOU Kang-gen, WU Ye-hui-zi, ZHANG Xue-kai, PENG Chang-hong, CHENG Yu-yao, CHEN Wei. Removal of Zn(II) from manganese−zinc chloride waste liquor using ion-exchange with D201 resin [J]. Hydrometallurgy, 2019, 190: 105171.

[19] BRUGGER J, MCPHAIL D C, BLACK J, SPICCIA L. Complexation of metal ions in brines: Application of electronic spectroscopy in the study of the Cu(II)−LiCl−H_2O system between 25 and 90 °C [J]. Geochimica et Cosmochimica Acta, 2001, 65: 2691−2708.

[20] SENANAYAKE G, MUIR D M. Competitive solvation and complexation of Cu(I), Cu(II), Pb(II), Zn(II), and Ag(I) in aqueous ethanol, acetonitrile, and dimethylsulfoxide solutions containing chloride ion with applications to hydrometallurgy [J]. Metallurgical Transactions B, 1990, 21: 439−448.

[21] MARLEY N A, GAFFNEY J S. Laser Raman spectral determination of zinc halide complexes in aqueous solutions as a function of temperature and pressure [J]. Applied Spectroscopy, 1990, 44: 469−476.
[22] QUICKSALL C O, SPIRO T G. Raman spectra of tetrahalozincates and the structure of aqueous $ZnCl_4^{2-}$ [J]. Inorganic Chemistry, 1966, 5: 2232−2233.
[23] SONG Le-xin, YANG Jing, BAI Lei, DU Fang-yun, CHEN Jie, WANG Mang. Molecule−ion interaction and its effect on electrostatic interaction in the system of copper chloride and *β*-cyclodextrin [J]. Inorganic Chemistry, 2011, 50: 1682−1688.
[24] DUDEV T, LIM C. Tetrahedral vs octahedral zinc complexes with ligands of biological interest: A DFT/CDM study [J]. Journal of the American Chemical Society, 2000, 122: 11146−11153.
[25] LI G S, CAMAIONI D M, AMONETTE J E, ZHANG Z C, JOHNSON T J, FULTON J L. $[CuCl_n]^{2-n}$ ion-pair species in 1-ethyl-3-methylimidazolium chloride ionic liquid−water mixtures: Ultraviolet-visible, X-ray absorption fine structure, and density functional theory characterization [J]. The Journal of Physical Chemistry B, 2010, 114: 12614−12622.
[26] de VREESE P, BROOKS N R, van HECKE K, van MEERVELT L, MATTHIJS E, BINNEMANS K, van DEUN R. Speciation of copper(II) complexes in an ionic liquid based on choline chloride and in choline chloride/water mixtures [J]. Inorganic Chemistry, 2012, 51: 4972−4981.
[27] PAGE M J, SOLDENHOFF K, OGDEN M D. Comparative study of the application of chelating resins for rare earth recovery [J]. Hydrometallurgy, 2017, 169: 275−281.
[28] ABBASI P, MCKEVITT B, DREISINGER D B. The kinetics of nickel recovery from ferrous containing solutions using an iminodiacetic acid ion exchange resin [J]. Hydrometallurgy, 2018, 175: 333−339.
[29] PEREZ I D, ANES I A, BOTELHO A B Jr, ESPINOSA D C R. Comparative study of selective copper recovery techniques from nickel laterite leach waste towards a competitive sustainable extractive process [J]. Cleaner Engineering and Technology, 2020, 1: 100031.
[30] ZHU Xiao-bo, LI Wang, ZHANG Chuan-xiang. Extraction and removal of vanadium by adsorption with resin 201*7 from vanadium waste liquid [J]. Environmental Research, 2020, 180: 108865.
[31] OKPALUGO T I T, PAPAKONSTANTINOU P, MURPHY H, MCLAUGHLIN J, BROWN N M D. High resolution XPS characterization of chemical functionalised MWCNTs and SWCNTs [J]. Carbon, 2005, 43: 153−161.
[32] FINŠGAR M. EQCM and XPS analysis of 1,2,4-triazole and 3-amino-1,2,4-triazole as copper corrosion inhibitors in chloride solution [J]. Corrosion Science, 2013, 77: 350−359.
[33] CAO Jiao-jiao, GUO Cheng-bin, GUO Xing-peng, CHEN Zhen-yu. Inhibition behavior of synthesized ZIF-8 derivative for copper in sodium chloride solution [J]. Journal of Molecular Liquids, 2020, 311: 113277.
[34] VANEA E, SIMON V. XPS and Raman study of zinc containing silica microparticles loaded with insulin [J]. Applied Surface Science, 2013, 280: 144−150.

色层分离法回收锗氯化蒸馏高氯残液中的 Zn(II)和 Cu(II)

吴业惠子[1]，周康根[1,2]，陈 伟[1,2]，雷清源[1]，张二军[1]，
程钰尧[1]，江 洋[1]，彭长宏[1,2]，江 钧[1]，张雪凯[1,3]

1. 中南大学 冶金与环境学院，长沙 410083；
2. 中南大学 国家重金属污染防治工程技术研究中心，长沙 410083；
3. 中南大学 化学化工学院，长沙 410083

摘 要：基于 Zn^{2+}/Cu^{2+}与 Cl^-配位能力的差异，采用阴离子交换色层分离法和 717 树脂，选择性回收氯化蒸馏提锗工艺所产生高氯残液中的锌和铜。理论计算和光谱分析表明，Zn^{2+}与 Cl^-的配位能力远强于 Cu^{2+}与 Cl^-的配位能力，同时 Cl^-浓度显著影响 Zn(II)和 Cu(II)在溶液中的存在形态。此外，考察 Cl^-浓度、树脂用量、振荡速率及温度等因素的影响，在优化条件下 Zn/Cu 两者间的分离因子达到 479.2。吸附等温线、吸附动力学、SEM、FTIR 和 XPS 等研究结果表明，该过程是均匀的单分子层化学吸附。最后，通过连续吸附柱实验分别回收高氯残液中的 Zn(II)和 Cu(II)，从而实现残液中废酸和锗的再利用。

关键词：色层分离；Zn/Cu 回收；高氯残液；阴离子交换；717 树脂

(Edited by Wei-ping CHEN)